Open Archive Toulouse Archive Ouverte (OATAO)

Low velocity impact modelling in laminate composite panels with discrete interface elements

Christophe Bouvet [a,*], Bruno Castanié [a], Matthieu Bizeul [b], Jean-Jacques Barrau [a]

[a] Université de Toulouse/UPS/LGMT, 118 route de Narbonne, 31062 Toulouse cedex 04, France
[b] Université de Toulouse/ISAE/DMSM, 10 av. E. Belin, 31055 Toulouse cedex 04, France

Impact
Interface
Matrix crack
Delamination
Modelling

ABSTRACT

A model enabling the detection of damages developing during a low velocity/low energy impact test on laminate composite panels has been elaborated. The ply model is composed of interface type elements to describe matrix cracks and volumic finite elements. This mesh device allows to respect the material orthotropy of the ply and accounts for the discontinuity experimentally observed. Afterwards delaminations are described with interfaces similar to the ones observed with matrix cracks and the coupling between these two damages are established. In the first step, simple stress criteria are used to drive these interface type elements in order to assess the relevance of model principle. Nevertheless, the well known problem of mesh sensitivity of these criteria prevents the use of this model for now as a predictive tool but rather as a qualitative tool. An experimental validation is carried out thanks to impact experimental tests performed by Aboissiere (2003) and a very good match has been found. However, this model could predictivelly be used and would allow to foresee an original method to detect delaminations during an experimental test. This modelling has been successfully tested experimentally and compared to a C-Scan ultrasonic investigation.

1. Introduction

Composite materials are being increasingly used in airframe and spatial applications thanks to their interesting mechanical characteristics and low specific weight. Nevertheless, for structures submitted to low energy impacts or minor objects drop, like tools during assembly or maintenance operation, composite laminates reveal a brittle behaviour and can undergo significant damages in terms of matrix cracks, fibres breakages or delamination. These damages are particularly dangerous because they drastically reduce the residual mechanical characteristics of the structure, and at the same time can leave very little visible mark onto the impacted surface. Many authors have consequently studied the impact behaviour of composite structures and their effects on residual strength, both experimentally (Abrate, 1998; Aoki et al., 2006; Petit et al., 2007; Davies and Olsson, 2004; Kwon and Sankar, 1993 . . .), as well as numerically (Allix and Blanchard, 2006; Choi and Chang, 1992; Finn and Springer, 1993; Li et al., 2006; De Moura and Gonçalves, 2004; Guinard et al., 2002; Hou et al., 2001 . . .), but a lot of work is still necessary to improve the modelling of the damage developing during impact on composite laminates to better assess

numerically their residual mechanical characteristics in order to optimise their design.

The first step to achieve in order to numerically design composite structures is the modelling of the impact and in particular the impact damages like matrix cracks, fibre/matrix debonding, delamination or fibres breakage. These damages are classically divided in two parts:

- The intralaminar damages, i.e. the damages developing inside the ply like matrix cracking, fibre/matrix debonding or fibres breakages.
- The interlaminar damages, i.e. the damages developing at the interface between two consecutive plies, namely delamination.

When these two damage types are considered separately, they are globally well understood and well simulated. The first ones, the intralaminar damages are often modelled thanks to damage internal variables (Allix and Blanchard, 2006; Li et al., 2006) or more rarely thanks to fracture mechanics (De Moura and Gonçalves, 2004). These different models seem to be in correlation with experimental observations and properly explain the physical phenomena of the different damages appearing inside ply. The second ones, the interlaminar damages are principally modelled thanks to interface type elements driven by damage internal variables (Allix and Blanchard, 2006) or thanks to fracture mechanics (Li et al., 2006; De Moura and Gonçalves, 2004; Collombet et al., 1996). These different

author. Address: Université Paul Sabatier, Filière Génie Mécanique, Bât. 3PN 118, route de Narbonne, 31062 Toulouse cedex 04, France. Tel.: +33 (0) 5 61 55 84 26; fax: +33 (0) 5 61 55 81 78.
E-mail address: bouvet@lgmt.ups-tlse.fr (C. Bouvet).

models seem to be in correlation with experimental observations and explain the physical phenomenon of the delamination creation. But the main problem of the physical understanding of the impact damages formation is the interaction which exists between the two damage types inside and between plies. The key point of impact damage formation modelling is these interaction, consequently this article will focus on this specific issue.

An interesting physical explanation of this interaction is proposed by Renault (1994). In this work, he proposes an experimental scenario of the different damages developing in a composite during a low velocity/low energy impact test. This scenario proposes to give matrix cracks a precursor role regarding the development of specific delamination. This idea is globally admitted in the literature (Abrate, 1998; Davies and Olsson, 2004; Allix and Blanchard, 2006). However this scenario begins with the development of matrix cracks in the impact zone below the impactor (Fig. 1). These cracks, of transverse direction (in (l, t) plane, where l is the longitudinal or fibres direction and t the transverse one) grow up during the loading following the fibre direction. Therefore, in each ply, a strip of fibres and resin disjoints and slides in the normal direction of this ply (z) (Fig. 1). This disjointed strip creates an interlaminar zone of tension stress between two consecutive plies and is susceptible to induce in this zone the formation of a delamination. In Fig. 1a, a schematic application of this scenario is proposed with a [−45°, 0°, 45°] stacking sequence, where −45° is the lower ply and 45° the upper ply. This stacking sequence is not a real one but represents only a part of a real stacking. In Fig. 1a, the disjointed strips of the first two plies are drawn and illustrate the interlaminar zone of tension stress. This zone, limited by the disjointed strips of the two adjacent plies, has a triangular shape with a size which grows from the impacted side to the non-impacted side. Fig. 1b illustrates the interlaminar zones of tension stress between the −45°/0° and 0°/45° plies.

Another explanation of this interaction has been proposed by Choi and Chang (1992) who explained the formation of a delamination by two main phenomena (Fig. 2):

- The first one is the delamination induced by inner shear cracks. A shear matrix crack located in the inner plies of the laminate generates a substantial delamination along the bottom interface and a small confined delamination along the upper interface of the cracked plies.

- The second one is the delamination induced by a surface bending crack. A bending matrix crack located at the surface ply of the laminate generates a delamination along the first interface of the cracked ply.

These two damages scenarios underline the fundamental role played by the interaction between these two damages which exists during the impact damage progression. Consequently this interaction must be taken into account in modelling to correctly simulate the experimental observations. To account for this interaction, many solutions have been suggested in the literature.

For instance one put forward by Choi and Chang, with reference to the impact damage scenario mentioned above, has used a very interesting delamination criterion evaluated only with mean stresses of the upper (noted $n + 1$) and lower (noted n) plies (z is the interface normal direction):

$$D_a \cdot \left[\left(\frac{\tau_{tz}^{n+1}}{S_i^{n+1}} \right)^2 + \left(\frac{\tau_{lz}^n}{S_i^n} \right)^2 + \left(\frac{\sigma_t^n}{Y^n} \right)^2 \right] = 1 \tag{1}$$

where τ_{tz}^{n+1} is the shear stress in the upper ply with t and z, respectively, the transverse and normal direction of the considered ply, τ_{lz}^n and σ_t^n, respectively, the shear and normal stress of the lower ply expressed in the considered ply reference, S_i^n and S_i^{n+1} the in situ interlaminar shear strength, respectively, in the lower and upper plies and Y^n the in situ transverse tensile or compressive strength in the lower ply. The two first terms in the square brackets represent the effects of a shear matrix crack on the creation of a delamination. These terms allow to account for the phenomena named by Choi and Chang "the delamination induced by inner shear cracks" (top of Fig. 2). The first term in τ_{tz}^{n+1} stress characterizes more specially the opening in fracture mode I of the delamination due to the shear matrix cracks of the upper ply and the second term in τ_{lz}^n stress characterizes the propagation in fracture mode II of the delamination due to the important stiffness in the longitudinal direction (due to fibres) of the lower ply. This last phenomenon is meant to explain, according to the authors, the propagation of delamination in the fibres direction of the lower ply.

The third term in the square brackets represents the effects of a matrix transverse crack on the creation of a delamination in the upper interface. This term allows to account for the phenomenon
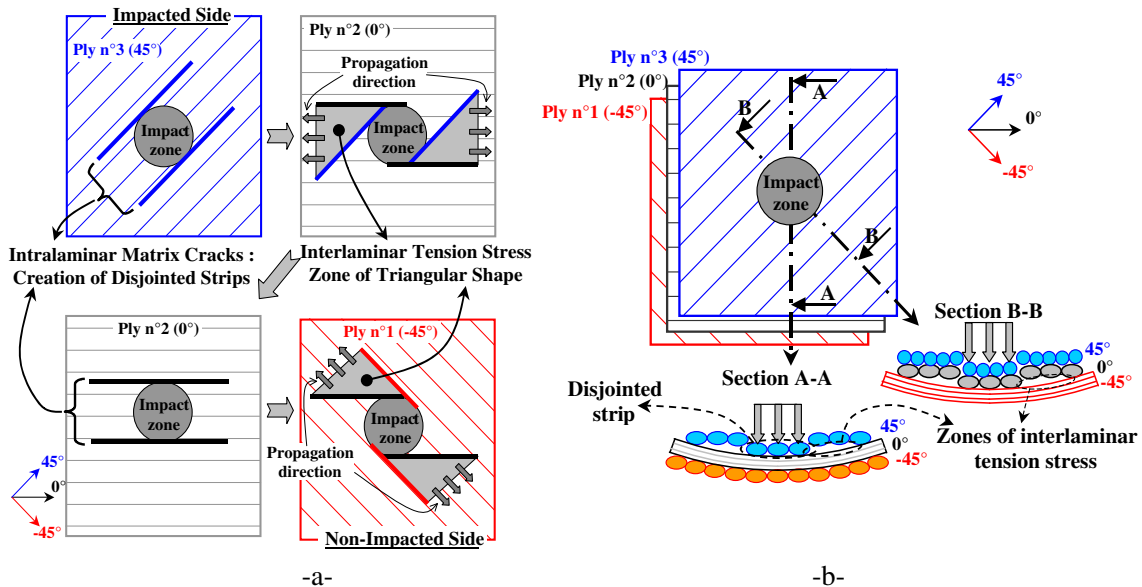

Fig. 1. Formation mechanism of delaminations (a) and interface tension stress zones (b).
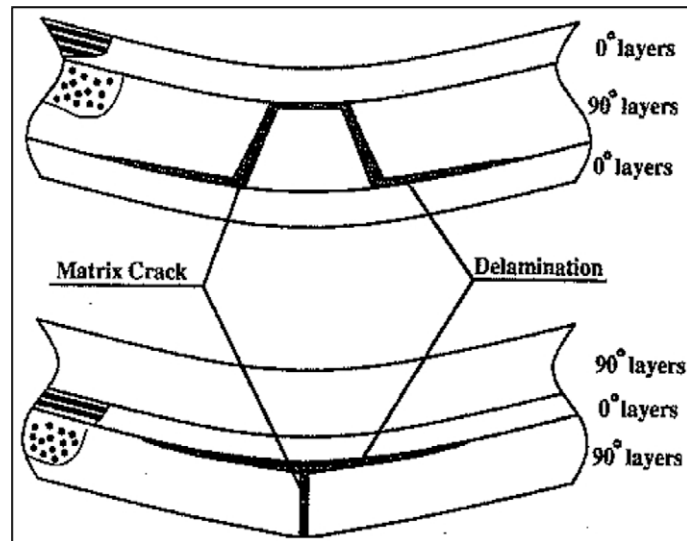
Fig. 2. Impact damage mechanisms. Top: delamination induced by inner shear cracks. Bottom: delamination induced by surface bending crack.

named by Choi and Chang "the delamination induced by surface bending crack" indicated at the bottom of Fig. 2.

And the D_a parameter is an empirical coupling coefficient to account for the precursor effect of the matrix cracking on the delamination which is practically taken equal to 1.8. Then the quadratic delamination criterion written inside the square brackets is considered reached if it equals 0.56 $(1/D_a)$ in presence of matrix cracks and if it equals 1 in their absence. However this delamination criterion is only assessed if a matrix cracking has been detected in the lower or upper ply, the matrix cracking being classically evaluated by the help of a stress quadratic function. Then for this criterion, the presence of matrix crack is necessary before the delamination formation. The authors have concluded that model prediction is in correlation with test data on different stacking sequences.

One drawback of this criterion is the different role played by the lower and upper ply. We want to point out that this designation of a lower or upper ply is purely artificial and in the model proposed in this paper, which is only partially influenced by this criterion, an equivalent role is played by lower or upper ply. But in addition we want to demonstrate that it is the bending effect induced by an impact which gives the lower plies a more important role in delamination progression.

Another problem of the model is that it detects only the delamination onset and does not account for the degradation due to it which can be a limitation for other bigger delamination area. In this article, the modelled delamination areas are practically less than 1000 mm². Then to represent the degradations due to delamination and to completely simulate the impact damages, an interface element seems to be necessary. Consequently, in the present model, an interface element with a total degradation possibility is elaborated.

This idea is equally used by Allix and Blanchard (2006) which are looked at an interface element driven by three damage internal variables; the first one, representing the damage created by the normal stress, is associated with the first mode of fracture, and the other two, representing the damage created by the shear stresses, are associated with the second and third modes of fracture. Then a non-associated damage evolution law is introduced to substitute these three damage internal variables with only one damage variable. The intraply damage is simulated with a similar way thanks to three damage internal variables, one for the matrix cracks in transverse direction, one for the in-plane shear matrix cracks and one for the fibres breakages. Then experimental evolution laws are introduced to drive these three damage internal variables. Finally, in this model, many couplings have been introduced between the variables of intraply damages and the ones for delamination but no coupling is explicitly written between these two damage types.

Afterwards this model is used to simulate the failure of holed sandwich structures and shows good match with experimental results monitored but it shows a problem to simulate the creation of delamination during an impact test. The authors conclude that due to the complexity of the phenomena involved in what is called delamination, the identification of the interface is still in its early stage.

Li et al. (2006) have used failure mechanics to simulate the delamination in a laminated panel and a pipe during an impact test. The energy release rates are evaluated thanks to VCCT (Virtual Crack Closure Technique) methods and the transverse matrix cracking damage is taken into account thanks to a degradation of the strength modulus. The simulations are in correlation with experiment even if the stacking sequences are particularly simple. Afterwards, the authors have underlined the difficulty to implement this model in a commercial FE (Finite Element) code because it requires accessing and transmitting information between elements in the neighbourhood of the delamination front which is a problem equally met in the implementation of the proposed model. Finally they have proposed the use of decohesive interfaces between sub laminates, whose properties are degraded as described by a damage variable in the context of continuum damage mechanics. This model has been applied to a few slightly different problems, like DCB (Double Cantilever Beam) tests, but its applicability to more sophisticated scenarios, such as modelling the damage in impact problem is yet to be explored which is seen as next phase of development.

Moura and Gonçalves (2004) have equally built an interface element with a softening behaviour between the three stresses; one normal and two shear stresses; and the three corresponding displacements. The coupling between these three damage variables is made simply thanks to linear interpolation which allows to simulate the fracture mixed modes and the area under the softening curve is classically linked to the energy release rate (Mi et al., 1998). These interface elements are equally used to account for the matrix cracking in the transverse direction. This idea, rarely

used in the literature, seems to be very interesting because it allows to simply introduce the interaction between intra and inter plies damages and consequently is suggested in the proposed model.

Afterwards, these interfaces are included in a laminate panel mesh but only where damages were detected during an experimental test which is of course a limitation for a predicting model. The simulations are quite in accordance with experiments even if the delamination is overestimated and the matrix cracks underestimated. According to the authors, these differences can be attributed to the mixed-mode damage model used and to the inter/intralaminar values of fracture mechanics characteristics which are considered identical. However, the apparent simplicity of the stacking sequences does not allow to test the predictive capacity of this model.

Collombet et al. (1996) have equally used an interface element driven by a simple criterion in normal stress which is implemented in an explicit FE code. The simplicity of the delamination criterion driven only with normal stress is explained by the big importance given to the first opening mode of fracture compared to the second and third fracture modes. This hypothesis is difficult to be experimentally tested and is largely discussed in the literature but it is used in the proposed model because it enables a very good delamination prediction comparing to experimental results. More experimental investigations are yet necessary to be done to evaluate the influence of each fracture mode on delamination formation.

Afterwards, in the modelling of Collombet et al., the matrix cracking is taken into account by a simple transverse stress criterion and the coupling between inter and intra laminar damage is imposed by a precursor role of the matrix cracks: a delamination is possible only if the lower ply is saturated in the matrix cracking. The comparison between experiment and simulation is quite in accordance even if the apparent simplicity of the stacking sequence does not allow to test the predictive capacity of this model.

Before concluding on this brief review of a few impact models, one is going to focus on two works dealing specially with the interaction between the inter and intraply damages.

Ladevèze et al. (2006) have studied the bridge between the mesomodel of impact damage mentioned above (Allix and Blanchard, 2006) and a micro model in microscale. Their main conclusion is that the mesomodel can be interpreted as the homogenized result of micro model. Thanks to this homogenisation, they have assessed the influence of intraply micro damage on the inter ply meso damage, i.e. the interaction between the intra and inter plies damages. They have concluded in particular that intralaminar damages have a negligible influence on interface damage under normal stress loading but a major role under shear stress loading. This conclusion is in correlation with experimental scenario of Renault (1994) who has given to shear matrix cracks and consequently to shear stresses a major role on the delamination formation. This idea has been largely used for the model building.

Then the authors have concluded that in their opinion a more specific link between delamination and transverse cracking must be derived.

A work with similar conclusions has equally been performed by Lammerant and Verpoest (1996). In their approach, they have modelized a laminate panel with volumic elements and damage springs for matrix cracks, as well as for delamination cracks. These damage spring elements are driven by critical energy release rate in mixed mode with linear interaction. The energy release rates are identified for 0°/0°, 0°/90° and −45°/45° interfaces and for intraply matrix cracks. They have studied only the propagation of these damages, i.e. initial damages are first present in the structure. They have shown in particular that the delamination shape depends strongly on the first matrix cracks and have concluded

that the existence of matrix cracks cannot be neglected when calculating the delamination development. This idea is present in the proposed model even if the cases of initiation and propagation of delamination are distinguished. In fact the existence of precursor matrix cracks seems to be necessary for a delamination initiation but not for its propagation.

Before concluding from this bibliography, which is of course not exhaustive, the authors invite the interest readers to consult review papers of Abrate (1998) or Davies and Olsson (2004).

The conclusions which are made from this bibliography are the following:

- An interface element is necessary to correctly simulate a delamination and in particular its degradation.
- An interface element is necessary to correctly simulate matrix cracks. Indeed we think that a continuum degradation model of the ply cannot take into account the effect of the matrix crack on the delamination. This important remark, which can be proved, is in our opinion the reason of an appropriate model derived from experiment.
- A coupling between the intra and inter ply damages is necessary and informations must be exchanged between the interfaces elements of the matrix cracks and delamination.

Then the aim of this work is to build a FE model which allows to account for these different remarks:

- Interface elements are used to simulate delamination.
- Interface elements are used to simulate matrix cracks in each ply and consequently the FE mesh must respect the fibres direction of each ply.
- The FE proposed allows the discussing between these two interface element types in order to account for the interaction between delamination and matrix cracks.

Finally this model is used to simulate experimental impact tests performed by Aboissiere (2002, 2003) on laminate composite 100×150 mm^2 plates simply supported by a 75×125 mm^2 shadow (IGC04.26.383^{N-4} Airbus) with a spherical impactor of 16 mm diameter. The material used is a prepreg with carbon unidirectional fibres and epoxy matrix HTA/EH24 manufactured by HEXCEL of around 0.25 mm thickness ply. The material characteristics evaluated by test are summarized on Table 1. Where E_l and E_t are the Young Modulus in longitudinal and transverse direction, respectively, v_{lt} the Poisson ratio, ε_l^f the failure strain in longitudinal direction, σ_t^f the failure stress in transverse direction, G_{lt} the shear modulus, τ_{lt}^f the failure shear stress and G_I the critical energy release rate obtained in propagation with a 0°/0° interface.

Among the numerous experimental investigations in the literature (Aoki et al., 2006; Davies and Olsson, 2004; Petit et al., 2007; Kwon and Sankar, 1993 ...), Aboissiere's work (2002, 2003) was used to set this model because of the following interests:

Firstly, the main stacking sequence used in these tests $[0°_2, 45°_2, 90°_2, -45°_2]_S$ respects the classical stacking laws, as the mirror symmetry and no angle exceeds 45° between two consecutive plies. This stacking is very simple, but does not allow to have a too complicated model; other model verifications are in progress in more specific industrial sequences.

Table 1
Material parameters.

E_l (GPa)	E_t (GPa)	v_{lt}	ε_l^f (%)	σ_t^f (MPa)	G_{lt} (GPa)	τ_{lt}^f (MPa)	G_I (N/m)
143	100	0.29	1.357	80	5.1	77	280 ± 50

Secondly, the damage observations, in particular delaminations, were realised with ultrasonic investigation of high quality (Fig. 13) which allows to simply identify each interface. On top of that, C-Scan was equally performed on the non-impacted side (Fig. 13b) which gives supplementary informations on the delamination shape and in particular the exact shape of the first interface of non-impacted side.

2. Numerical modelling principle

In our opinion and according to the concluding remarks mentioned above, the FE modelling of each ply of the composite laminate panel must account for the discontinuity created by matrix cracks and in particular by shear matrix cracks. Consequently the ply mesh must respect the exact material orthotropy in order to allow for the creation of these cracks. These matrix cracks are globally created by three stress components (Fig. 3):

- A transverse stress (σ_{tt}) which creates cracks normal to transverse direction (t).
- A out-of-plane shear stress (τ_{tz}) which creates cracks inclined of about $\pm 45°$.
- And an in-plane shear stress (τ_{lt}) which creates cracks normal to transverse direction (t).

In order to respect at best these cracks direction, the ply is meshed in little strips in the longitudinal direction with one volumic element in its width and thickness of the ply (Fig. 4). In this model, only inclined direction is not respected to avoid too complex modelling. This hypothesis seems reasonable if the ply thickness is small compared to the laminate thickness. Moreover, this hypothesis justifies equally the unique FE in the ply thickness.

Afterwards these little strips are connected together with interface type elements of null length (Fig. 4). There are practically not interface elements but spring elements which are used for the sim-

plicity of programming in the used FE code (SAMCEF®). The main difference between these two element types is that interface element can easily take into account the surface element which is very important for a specific non-homogeneous mesh. In our case, the proposed ply mesh imposes a homogeneous size mesh and these two element types are very similar but it is easier to develop spring element in a software like SAMCEF®.

Then null length springs of very high stiffness (typically 10^7 N/mm) are used to join together two consecutive strips and these stiffnesses are put to zero if matrix crack exists. In order to avoid numerical instabilities, the stiffnesses are cancelled progressively with time, and during this delay, the global displacement is kept constant. This classical way, to avoid instabilities, is similar to "delay effect" proposed by Allix and Blanchard (2006).

The matrix crack is derived from a classical quadratic equation:

$$\left(\frac{\langle \sigma_t \rangle^+}{\sigma_t^f}\right)^2 + \frac{\tau_{lt}^2 + \tau_{tz}^2}{\left(\tau_{lt}^f\right)^2} \leqslant 1 \tag{2}$$

where σ_t is the transverse stress, τ_{lt} and τ_{tz} the shear stresses in the (lt) and (tz) planes, $< >^+$ the positive value and σ_t^f and τ_{lt}^f the failure stresses mentioned above. A particularity of this model is to drive this matrix cracking criterion of these springs thanks to stresses in adjacent elements and not to stresses in the spring. Then, the criterion is evaluated in each volumic element of the ply, and a spring is broken if this criterion is reached in at least one of its 4 neighbouring volumic elements. For example, for the spring R_1 of the Fig. 4, the criterion is evaluated thanks to the mean stress in the 4 volumic elements E_1, E_2, E_3, E_4, and not to the force in the spring, which allows to avoid stress concentration at the tip of the matrix cracks. This criterion can be considered as an average stress criterion as the one proposed by Whitney and Nuismer (1974). In fact, this is similar to average stresses over a distance which depends on the mesh size. This mesh sensitivity will have to be further studied, nevertheless in the present simulated impact test, the matrix
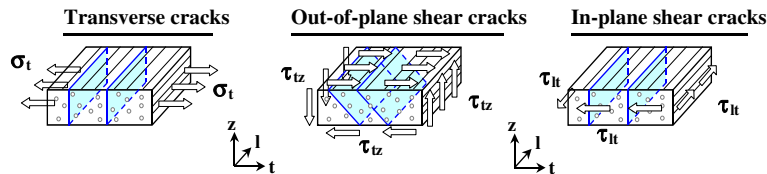

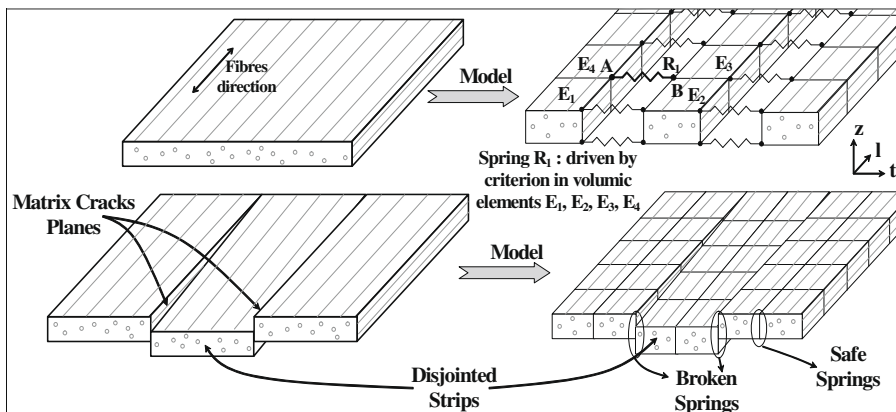**Fig. 3.** The three types of matrix cracks inner the ply.

Fig. 4. Model of the ply.

cracks revealed to be important especially for damage initiation and not for damage propagation. However we want to point out that this propagation is determinant in the final damage morphology.

This ply model enables to correctly take into account the proposed experimental observations in respecting the orthotropic behaviour of the ply, but it obliges to build a refined and fastidious mesh. In fact this model imposes a constant size of the FE mesh in the studied zone. Another particularity of this ply model is to impose a meshing for the $\pm 45°$ plies with a diamond-shaped element to allow for the coincidence between two consecutive plies (Figs. 7 and 8). Therefore only stacking sequences with 0°, 90° and $\pm 45°$ plies can be meshed, which is not a limit because most industrial applications are of this type.

In this model, the fibres failure is equally taken into account because this damage can cause drastic decreasing of material stiffness in the fibres direction. It is classically simulated at each Gauss point of volumic elements with a strain failure criterion:

$$\varepsilon_l \leqslant \varepsilon_l^f \tag{3}$$

where ε_l is the strain in the fibre direction and ε_l^f is given in Table 1. When this criterion is reached, the longitudinal Young modulus E_l and the shear modulus G_{lt}, G_{tz} and G_{lz} are drastically decreased, practically divided by 20 to avoid numerical instability. This fibre criterion, which can seem secondary compared to delamination criterion, strongly influences the delamination propagation in particular in the 90° direction during the impact test mentioned below (Fig. 17).

When the different plies are meshed with volumic and matrix cracks spring elements, springs are added to join them together and allow delamination (Fig. 5).

Therefore these delamination spring elements have the following properties; if no interface cracks exist, two consecutive plies are attached together with four null length springs of very high stiffness (typically 10^7 N/mm in the three directions) otherwise the stiffness is put to zero (Fig. 5). And to avoid numerical instabilities during the cancellation of stiffness, the "delay effect" (Allix

and Blanchard, 2006), similar to the one presented above for matrix crack, is implemented.

In fact, four springs are necessary (Fig. 6a), because there are two nodes for the upper ply and two nodes for the lower ply. Then each spring makes the bonding between one upper ply node and one lower ply node. Physically, each spring represents one quarter of the delamination concerned surface (Fig. 6b). For example, in Fig. 6b, the spring R_1 between the nodes A and D represents the surface R_1. Now a criterion must be defined to drive interface crack spring and to simulate the delamination. Two approaches are classically possible, one in fracture mechanics with a criterion in energy release rate and another one in limit stress. In the actual
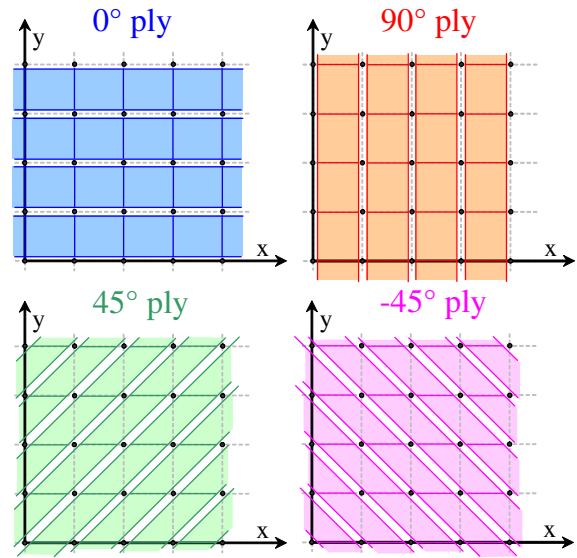

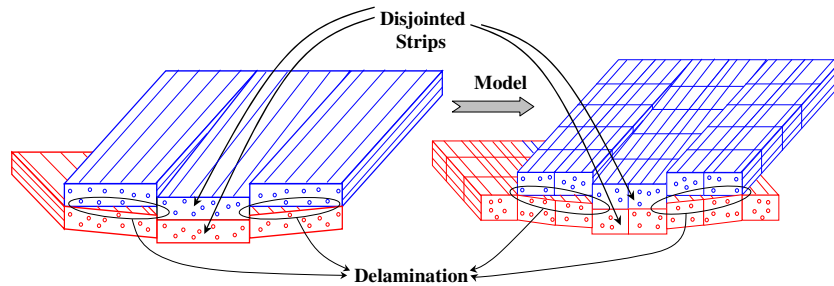**Fig. 7.** The four mesh types of 0°, 90°, 45° and −45° plies.
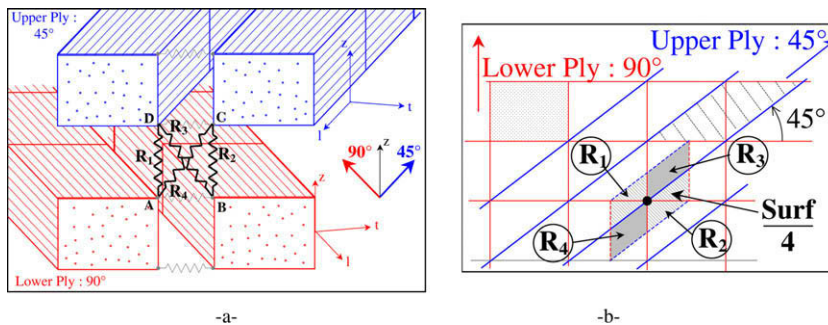

Fig. 5. Model of the interfaces.

Fig. 6. The four springs of delamination (a) and the covered surface (b).
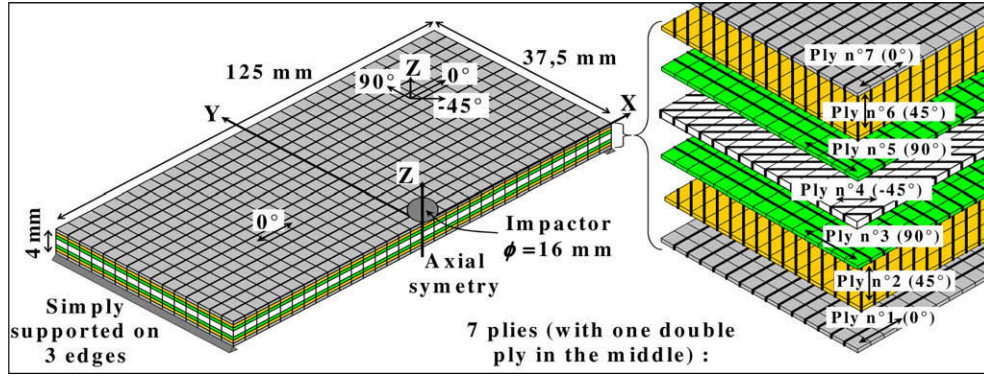
Fig. 8. Finite element mesh.

model, a limit stress criterion is implemented for its simplicity and an energy release rate criterion is actually studying. This choice of very simple criterion was made in the first step in order to assess the relevance of model principle. Nevertheless the well known problem of mesh sensitivity (Mi et al., 1998) of this criterion prevents the use of this model for now as a predictive tool but rather as a qualitative tool. The main objective of this model is by the way the physical understanding of the impact damage creation rather than the predictive model building.

On top of that, with regard to the bibliography remarks and in particular the experimental delamination scenario proposed by Renault (1994), only the interlaminar normal stress is considered in the criterion. This hypothesis neglects the second and third fracture modes as regard to the first opening mode of fracture. With this hypothesis, good results on delamination morphology compared to the experiment are obtained.

This result, which is confirmed by other authors (Collombet et al., 1996), is of course available only for the considered impact test and is probably not applicable to other damage scenarios like impact on thick plates or tension of holed composite plates. So this delamination criterion is used:

$$\text{For } i = 1 \text{ to } 4: \quad \sigma_{zi} = \frac{F_{zi}}{Surf/4} \leqslant \sigma_{lim} \tag{4}$$

where σ_{zi} is the interlaminar normal stress in the z direction for the spring i, F_{zi} the force in the spring i, Surf the surface concerned with the group of four springs and σ_{lim} a limit stress of interface crack. This limit stress, fundamental for this model, is characteristic of the delamination initiation, with or without preliminary matrix cracking as well as its propagation. Then three delamination cases can be distinguished:

- The first case is the initiation which is defined by a delamination creation without preliminary damage. In this case the limit stress σ_{lim} is chosen equal to the matrix failure stress σ_t^f (80 MPa). But practically in every simulated test this criterion is never reached before the propagation one, which is coherent with the work performed by Choi and Chang.
- The second case is the propagation which is defined if a neighbouring delamination spring element is broken. Practically, each delamination spring has four neighbours and is considered in propagation if at least one of its four neighbours is broken. In this case, the σ_{lim} value has been identified thanks to the delaminated area measured experimentally: $\sigma_{lim} = 10.5$ MPa (Fig. 11b).
- The last case is a pseudo-propagation which is defined if a matrix cracking exists preliminary. Practically, each delamination spring is confounded with two matrix cracking springs, one for the upper ply and one for the lower ply. Then a delamination spring is considered in pseudo-propagation if at least one of these two matrix cracking springs is broken. In this case, the σ_{lim} value has been chosen equal to the propagation one: $\sigma_{lim} = 10.5$ MPa.

This value of σ_{lim} could seem very low compared to the matrix failure stress ($\sigma_t^f = 80$ MPa) but represents a different phenomenon: the failure propagation. So this limit stress should rather be related with the critical energy released rate ($G_I = 280\pm50$N/m) measured experimentally. In order to achieve this relation, a DCB test was simulated using this criterion. However to be representative of the impact test, two plies at 0° and 45° of 0.5 mm thickness were meshed and jointed together with delamination interface elements with the limit stress of 10.5 MPa above mentioned (Fig. 9). The force versus displacement curve can be obtained (Fig. 10a)
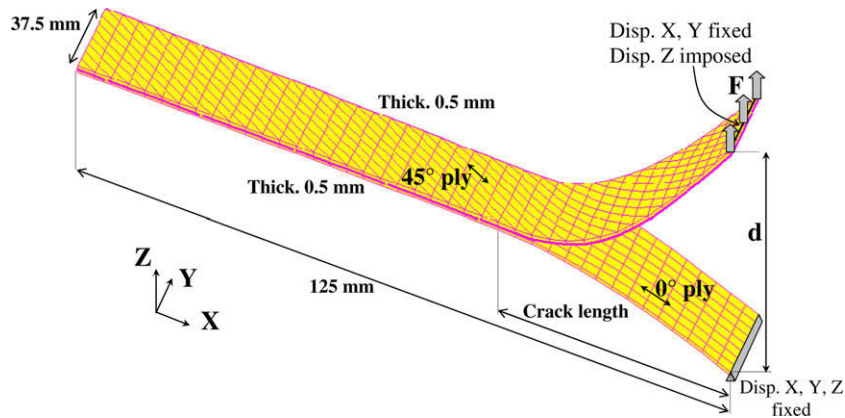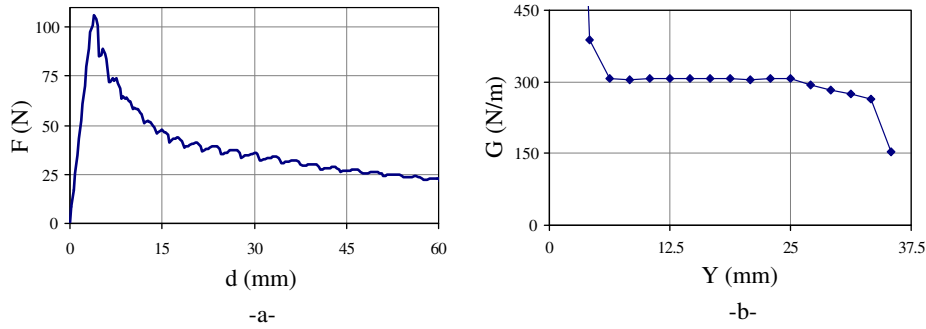

Fig. 9. DCB test.

Fig. 10. Force versus displacement curve (a) and critical energy release rate at the crack tip (b).

and a local calculation of the critical energy release rate with a VCCT method was made at the crack tip (Fig. 10b). This calculation was performed for each spring element, thanks to stress obtained just before failure and displacement just after, along the crack tip for a crack of about 60 mm length. Outside boundary effects (Fig. 10b) due to particular mesh, a constant critical energy release rate of about 300 N/m is obtained. This value is in correlation with the experimental value of 280 ± 50 N/m measured by Aboissiere and confirms the relevance of the used limit stress value. Due to the VCCT method, the fracture modes II and III were also evaluated, and this calculation showed that these two modes are less than 5% of the fracture mode I and can be considered negligible for this test.

However we want to underline that the critical energy release rate evaluated thanks to this numerical DCB test is of course mesh sensitive but is also sensitive to the stiffness of the structure. In fact, the energy release rate is dissipated in the "delay effect" of the springs as mentioned above, and depends totally on the local stiffness around the spring and therefore also on the local mesh. This calculation is only valid with the presented mesh and for this type of solicitation, therefore the same mesh is used for both the DCB test and the impact test. In particular, if this numerical DCB test is performed with another stacking sequence or with other plies thicknesses, the obtained critical energy release rate will be different, which is due to the stress monitoring of the criterion. To avoid that, softening springs should be used to drive the delamination propagation thanks to the critical energy release rate. In fact, the area under the stress/ displacement curves of these softening spring allows to indirectly introduce the energy release rate of the interface (Mi et al., 1998). In the present model, this factor is not taken into account and to avoid mesh size problem, all FE have the same size (about $2 \times 2 \times 0.5 \text{ mm}^3$) and the limit stress σ_{lim} was identified with reference to this mesh size. On top of that, as mentioned above, this mesh sensitivity prevents the use of this model for now as a predictive tool but rather as an understanding tool.

3. Experimental validation

Finally, this model was set up in the FE software Samcef® and Aboissiere's impact tests were simulated. A half composite plate is meshed with one volumic element by plies sequence of the same orientation, then seven elements in the thickness $[0°_2, 45°_2, 90°_2, -45°_4, 90°_2, 45°_2, 0°_2]$ with a double thickness element in the middle are presented. An axial symmetry condition around the z-axis is imposed (Fig. 8). Later in this paper, the term "ply" will be used for a plies sequence of the same orientation.

The mesh size in x and y directions is constant and equals to $2 \times 2 \text{ mm}^2$. The volumic elements are afterwards attached together by the discrete interface element mentioned above. In all, the FE model counts 135000 degrees of freedom and the calculation lasts for about 6 h on a PC dual core 3.5 GHz with 2 Gb of RAM but this size and this time should certainly be decreasing by optimising the programmation. Then non-linear static numerical calculation with an imposed displacement of the impactor is performed, since a lot of authors (Abrate, 1998; Kwon and Sankar, 1993) showed the static/dynamic equivalence for this type of low velocity/low energy impacts. The displacement of the impactor, which is meshed with infinite stiffness element, is imposed between 0 and 6 mm and to compare this result with experimental test, the equivalent impact energy is evaluated thanks to the integration of the displacement/ force curve. Then the maximum impact force versus equivalent impact energy curve is drawn in Fig. 11a and is compared to the experimental results. We want to point out that this comparison should be considered with caution because of the criterion mesh sensitivity mentioned above. However there is good correlation up to 15 J but deteriorates after, it is certainly due to the impactor perforation phenomenon which is not simulated in the present model. In particular the impactor's perforation creates fibres failures by out-of-plane shear stresses (τ_{lz}) which are not taken into account by the fibres failure criterion. The simulation should over-
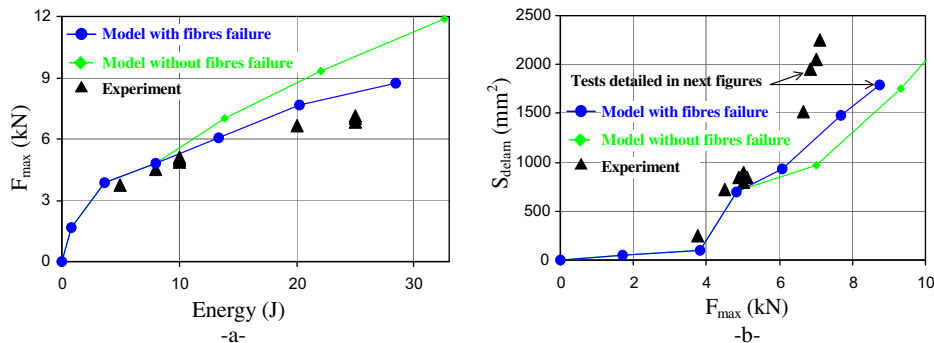

Fig. 11. Maximum impact force versus energy curve (a) and delaminated area versus maximum impact force curve (b).

estimate the impact force and could explain a part of the difference between the experiments and modelling.

Afterwards, the evolution of the delaminated area versus maximum impact force is drawn in Fig. 11b and is compared to the experiments. Like the previous case and for the same reason, the experimental and model curves are in accordance up to 6 kN but there is no proper match afterwards. We want equally to point out that this comparison should be considered with caution because it is this curve which has been used to evaluate the limit

stress σ_{lim} mentioned above. Moreover the limit stress used for delamination springs was identified due to this curve and the correlation allows only to verify the good identification of this parameter.

The different damage types given by the model are summarized in Fig. 12. At the left of this figure, the matrix cracking is drawn from the first ply, non-impacted side, to the seventh ply, impacted side. These matrix cracking damages show an axial symmetry imposed by the model, then the impact point is the central point of
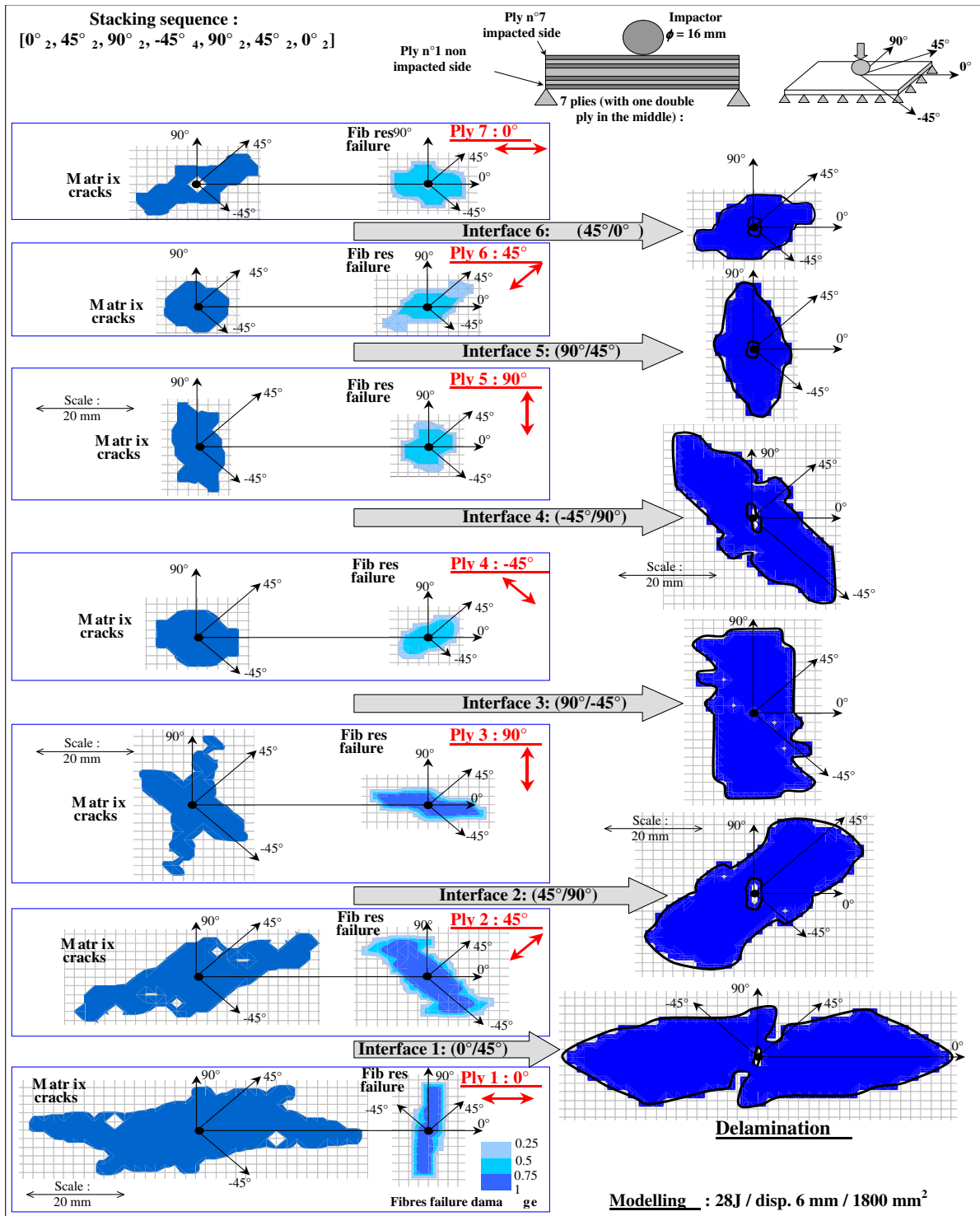

Fig. 12. Numerical modelling of matrix cracking, fibres failures and delamination for 6 mm displacement.

damage maps. These damage maps represent the matrix cracking indicator which equals 0 in safe material and 1 in damaged material. This indicator is evaluated for each matrix cracking spring and a constant value in thickness of the ply is imposed due to the adopted matrix cracking model. This damaged zone by matrix cracking is bigger in the non-impacted side than the impacted size due to flexion effects.

In the middle of this figure, the fibres failure is drawn from the first to the seventh ply. These damage maps represent the fibres failure indicator which equals 0 in safe material and 1 in broken material. This indicator is evaluated at each Gauss point of volumic elements which counts 8 Gauss points due to the used FE. The indicator's value is between 0 and 1 in mean per element. This damage is equally bigger in non-impacted side than impacted size due to flexion effects.

Finally at the right of this figure, the delamination damage is drawn for each interface. These damage maps represent the delamination indicator which equals 0 in safe interface and 1 in delaminated interface. This indicator is evaluated for each delamination spring and is taken equal for each group of four delamination springs mentioned above. Afterwards, in order to compare these delamination maps with experimental ones obtained by C-Scan, these delamination surfaces are brought together and filled with the colour obtained by C-Scan (Fig. 13).

In fact, to test for the relevance of a modelling, the global delamination area or the force/impact energy curve are insufficient, the morphology of the delaminated area of each interface gives much more information on the impact damage scenario. So the simulated delaminations are compared to the experimental one obtained by C-Scan at 25 J for experiment and 28 J for modelling (Fig. 13). The greatest value for the impact energy of the model is explained by the overestimation of the impact force mentioned above. Even if the mesh sensitivity of the delamination criterion mentioned above prevents to wholly appreciate the quantitative prediction of this model, in a definite way the qualitative comparison can be made and in particular the comparison of the delamination shape of each interface. The comparison between these two delamination pictures (Fig. 13) is very good, the proposed model allows to account for a lot of experimental observations:

Firstly the propagation of a delamination is always driven by the direction of the lower ply (Fig. 12). In fact, it is principally the tension in the fibre direction of the lower ply which creates the opening of the delamination fracture. This phenomenon is very well illustrated in Fig. 14. This figure represents the displacement field obtained by FE calculation at 6 mm displacement for two cross sections in 0° and 45° directions. It can be noted in these sections that only elements with fibres in the cross section direction are well represented. In fact, the other ones have no parallel sides to the section plan which gives a wrong impression of penetration between elements. Nevertheless, it can be seen on this picture the large opening of the last delamination between the 0° and 45° obtained numerically thanks to a cross section in the lower ply direction (here in 0° direction) and the relatively large opening of the previous delamination between the 45° and 90° thanks to a cross section in the lower ply direction (here in 45° direction).

To study more particularly this phenomenon, the displacement in z direction of the last ply is drawn versus the x-position (Fig. 15) for a cross section along 0° and 45° directions. It clearly appears on these curves a knee point at the location where the last (or the before last) delamination ends.

To confirm this result, an experimental test was performed in the laboratory with a carbon/epoxy prepreg material (T700/M21) and with the same stacking sequence. The main difference between this material and Aboissiere's lies in the resin which is a pure epoxy resin for Aboissiere and a mix epoxy resin with thermoplastic constituents for the M21. This test is similar to Aboissiere's but in static conditions to allow for the observations of the 3D shape of the last ply thanks to an image correlation system with two CCD cameras (Fig. 16a). That is we compare the experimental displacement field with the model at the same imposed displacement of 5 mm.

Afterwards the curves of z-displacement along 0° and 45° lines were drawn (Fig. 15) and compared with the model. These curves are in good fit for the 0° cross section as for the 45° cross section
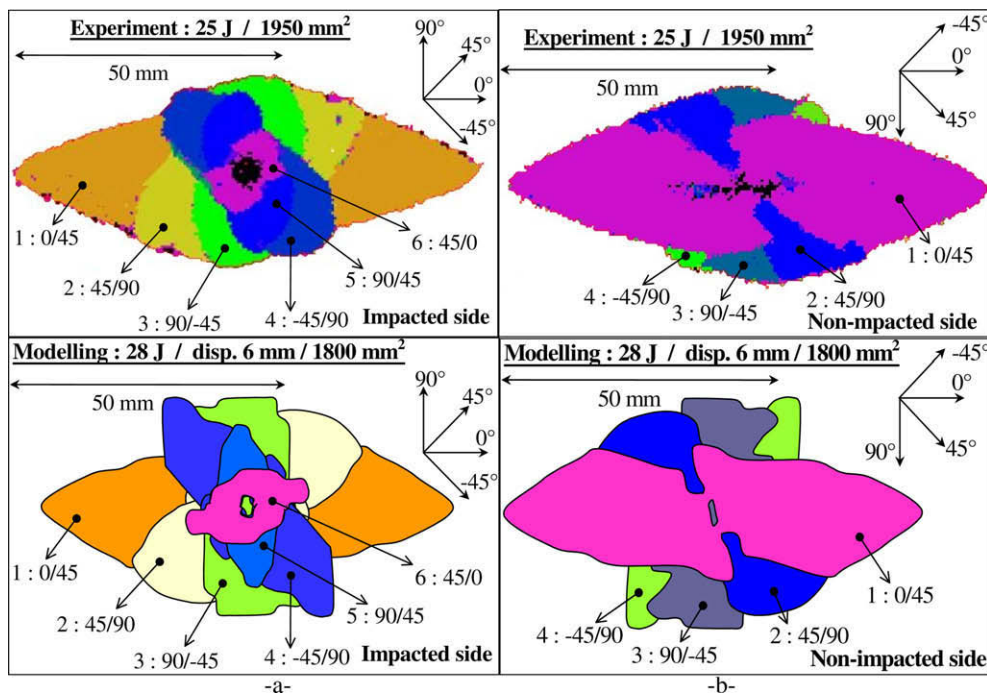

Fig. 13. Experimental and modelling delamination in the impacted (a) and non-impacted side (b).
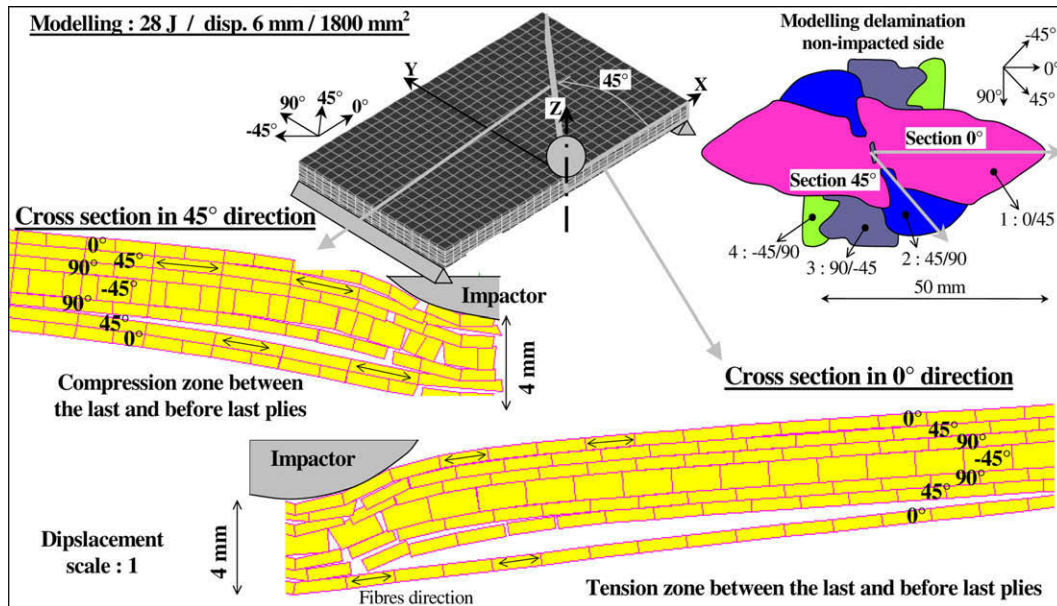
Fig. 14. Displacement response of the model.

and in particular the knee point foresaw by modelling is clearly observed experimentally which confirms the large opening of the delamination and in particular of the last one simulated by the model. So this test validates the model because its prediction was exactly foreseeable from the experimental test.

Afterwards, other experimental curves of z-displacement along different direction were drawn and enabled us to observe each time two knee points which are plotted on the z-displacement field (Fig. 16a). A criterion on the derivate of the z-displacement curve is used to evaluate automatically these points. Then this knee point curve is compared to a C-Scan performed on the non-impacted side of the laminate panel (Fig. 16b). The curve, evaluated thanks to knee points, is in very good agreement with C-Scan and allows to confirm the following method of delamination. Moreover it allows to observe the delamination evolution during the experimental test, contrary to C-Scan observation, which should normally give interesting supplementary informations on the damage formation. Other experiments must be carried out to confirm this method. Moreover, even if for instance this observation is performed during a static test, the use of two rapid cameras could allow us to perform this observation during a dynamic test. This procedure is actually in progress.

Secondly, the delaminations do not propagate (or propagate only slightly) in the upper ply direction of the impacted zone due to a compression zone (Fig. 14). This phenomenon is properly illustrated by the experimental C-Scan obtained on the non-impacted side (Fig. 13) which clearly shows the clamping of the delamination in the 45° of the impacted zone direction and it is well illustrated by the model.

Thirdly, the global direction of the projected delaminated area is strongly directed in the 0° direction (Fig. 13). This experimental observation is globally well taken into account by the model even if it gives a big delamination in the 90° direction. This is perhaps due to fibres failures which are imperfectly modelled by this model. It is not easy to experimentally confirm this hypothesis because fibres failure is very difficult to observe experimentally. Nevertheless micrographic cuts or deplying (Sztefek and Olsson, 2008) could allow to situate the fibres failure and to compare them with the modelling (Fig. 12).

Another possibility to indirectly confirm this hypothesis is to remove the fibre failures of the model. In Fig. 17, the delamina-

tion obtained without fibre failure is drawn, and the curves force/impact energy and delaminated area/maximum impact force are equally reported on Fig. 11. The lack of fibre failure increases the impact force and energy for the same imposed displacement, and for the same displacement of 6 mm the delaminated area increases strongly from 1800 to 2850 mm^2 (Fig. 17). However the delamination morphology is very different, the projected delaminated area is not yet directed by 0° direction but quasi-circular without the fibres failure (Fig. 17). The delamination propagation in the 90° direction is fast and stopped close to the boundary conditions. This phenomenon equally allows to better understand why the projected delaminated area is in the 0° direction. This is due to the rectangular shape shadow which preferentially induces fibre failures in the 45° and 90° directions, in the non-impacted side. Then, in the studied stacking sequence, the 45° and 90° plies (plies no 2 and 3), in the non-impacted side, break first (the 45° ply breaks before the 90° ply due to flexion effect), and decrease stresses in these directions which stops delamination propagation. At the same time, the last 0° ply (ply no 1) breaks very late during the impact test modelling. Practically, this ply is still safe until 5 mm displacement, which tends to propagate delamination in its direction. Now tests with different boundary conditions to check this result are under development.

Finally the proper resemblance between the experimental and numerical damage morphology allows us to conclude that the hypothesis used in this model are globally representative of the physical phenomena. In particular, this model can help to better understand the phenomenon of delamination formation during an impact test. In fact, three cases of delaminations are considered: Pure initiation, propagation and pseudo-propagation (cf. Section 2). As already mentioned above, the first case of pure initiation, i.e. a delamination without preliminary damage is never found in the different simulated impact tests. And the third case of pseudo-propagation, i.e. a delamination with preliminary matrix cracking is found only for one element (2 with the axial symmetry) of each interface. This case is necessary in the model to initiate the delamination but once it begins, the propagation phenomenon is always reached before the pseudo-propagation.

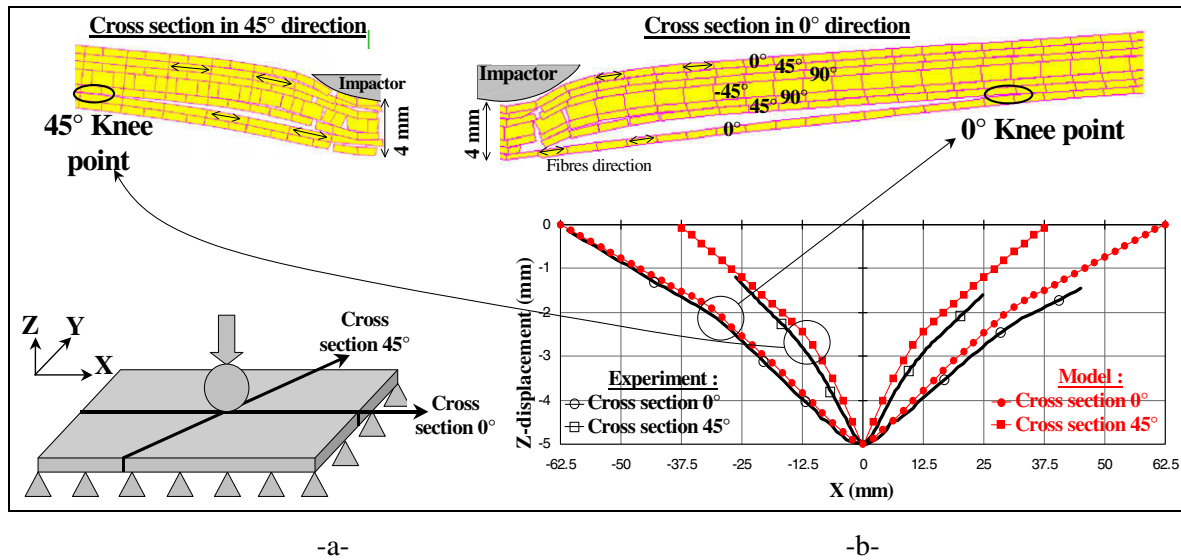This suggests two different types of matrix delamination formation:

Fig. 15. Z-displacement of the non-impacted side composite panel in the 0° and 45° directions.
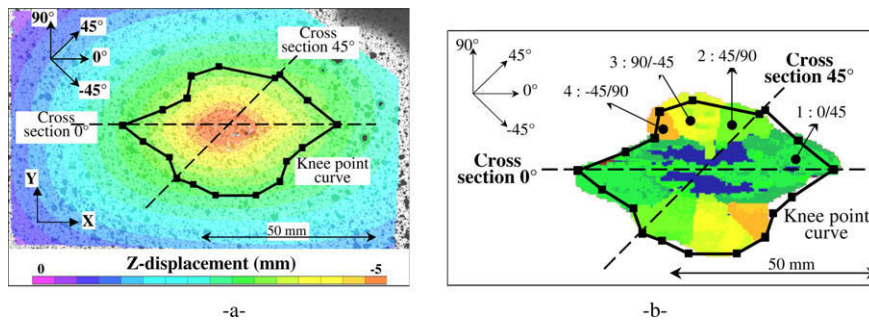

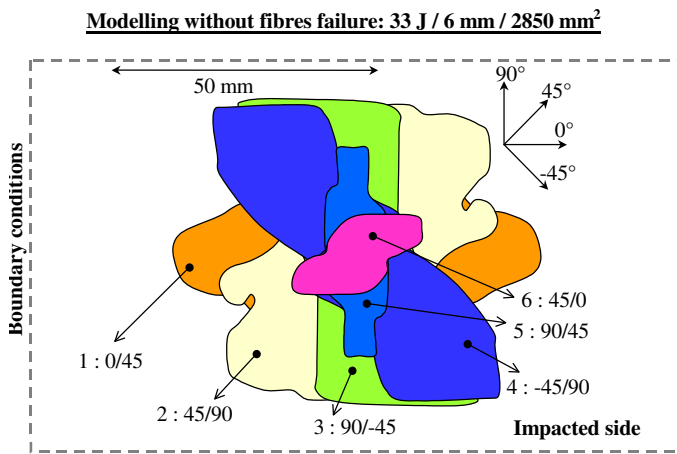**Fig. 16.** Knee point curve with z-displacement field (a) and with non-impacted side C-Scan (b).

Fig. 17. Modelling delamination without fibre failure impacted side.

- A delamination formation which corresponds to the delamination initiation: when a ply develops an important matrix cracking damage with safe interfaces and when these matrix cracks reach this interface, a delamination is initiated at this specific point. These matrix cracks can be created by normal stresses, which correspond to the surface bending cracks mentioned by Choi and Chang or by shear stresses, which correspond to the inner shear cracks mentioned by Choi and Chang (Fig. 2).

- A delamination formation which corresponds to the delamination propagation: when a disjointed strip is created by preliminary matrix cracking, a zone of tension stress is created and involves a delamination propagation in opening mode I fracture before the matrix cracking. This scenario corresponds to the one proposed by Renault (Fig. 1). It is particularly visible in Fig. 12 where the delaminated areas are bigger than the matrix cracked ones.

In a real laminate panel damaged by an impact test, the delamination initiation will be present in the zone directly under the impact point and the delamination propagates far from the impact point.

Consequently, it seems necessary to take into account these two types of delamination formation to correctly simulate the impact test damage.

4. Conclusion

An impact damage model has been set up to simulate the different damage types forming during an impact test on laminate composite panel. The main ideas used to build this model are:

- The matrix crack damage is modelized thanks to localized damage to take into account discontinuity created by this phenomenon.

- The delamination damage is modelized with interface type elements, and the failure criteria depends on the stresses of the interface but also on the stresses of the adjacent layers.
- The fibre failure is modelized thanks to continuum variable.

The main objective of this model is to better phycically understand the impact damage creation. In the first step, very simple criteria written with stresses, was used in order to test the relevance of fundamental ideas of this model. The well known problem of mesh sensitivity of these criteria limits for now the use of this model as a predictive tool.

Finally this model has been used to simulate experimental tests performed by Aboissiere (2002, 2003) and shows very good agreement with experiment for the global response of the structure as well as for the delamination morphology in each interface obtained by C-Scan. This good result allows to justify the used hypothesis and shows the relevance of this model. Then, it has been used to underline different points:

- The fibres failure is fundamental in the impact damage development and in particular the fibres failure in a direction locks the delamination propagation in this direction and induces it in the perpendicular direction. Experimental confirmation must be done to confirm this effect, for example the use of fibres with very different failure strain.
- The fracture mode I is fundamental on the delamination propagation. Indeed, the proposed model allows us to take into account the delamination with only an interlaminar normal stress criterion. Even if additional experiments must be done to study the effect of the fracture mode II on delamination propagation, the present model allows to clearly confirm the predominance of the fracture mode I on this phenomenon. Of course this result is true only for impact on this type of panel and may be inappropriate on other configurations like for example impact on thick panel or tension on holed panel.
- The displacement field of the last ply is influenced by the existence of the delamination and it is possible to evaluate the delaminated area during an indentation test thanks to an image correlation system with two CCD cameras. A correlation of this measure with a C-Scan allowed us to validate this method and other tests are in progress to confirm this result.

Now the fundamental ideas of this model were confirmed by the good relevance of the damage morphology, the different criteria should be improved to obtain a really predictive tool. The first point to study is the use of softening springs for delamination elements to eliminate the mesh sensitivity. This mesh sensitivity will be tested on different meshes, for delamination elements, as well as for matrix cracking elements. Another point to focus is the development of a new criterion for damage of fibres failure to better simulate the panel perforation. Finally the fracture mode II will be taken into account to modelize other damages types like impact on thick plate.

Afterwards this model will be used as an initial condition to simulate a test of compression after impact, indeed the loss of strength in compression is directly due to impact damage. But the initial shape of the panel after impact influence the residual compression strength and this model must be improved to simulate the permanent indentation after impact.

However this permanent indentation is a dominating parameter to certify a composite structure in the field of aeronautics. Since it is the damage tolerance concept: The structure must withstand ultimate loads with a permanent indentation smaller than the BVID (Barely Visible Impact Damage).

A lot of work is still necessary to wholly simulate the damage tolerance of a composite panel and to take into account, at the same time, the damage during impact and the permanent indentation to evaluate the residual strength and to optimise the design of composite structures in damage tolerance.

References

Aboissiere, J., 2003. Propagation de dommages d'impact dans un matériau composite stratifié à fibres de carbone et résine époxyde. Thesis of the University Paul Sabatier of Toulouse, France.

Aboissiere, J., Michel, L., Eve, O., Barrau, J.J., 2002. Matrix cracking and delamination under fatigue loading. ECCM10, Brugge, Belgium.

Abrate, S., 1998. Impact on Composites Structures. Cambridge University Press.

Allix, O., Blanchard, 2006. Mesomodeling of delamination: towards industrial applications. Composites Science and Technology 66, 731–744.

Aoki, Y., Iwahori, Y., Ishikawa, T., Kondo, H., Hiraoka K., 2006. Dent depth and CAI property of CFRP laminates subjected to low velocity impact. ECCM12, Biarritz, France.

Choi, H.Y., Chang, F.K., 1992. A model for predicting damage in graphite/expoxy laminated composites resulting from low-velocity point impact. Journal of Composite Materials 26 (14), 2134–2169.

Collombet, F., Bonini, J., Lataillade, J.L., 1996. A three dimensional modelling of low velocity impact damage in composite laminates. International Journal for Numerical Methods in Engineering 39, 1491–1516.

Davies, G.A.O., Olsson, R., 2004. Impact on composite structures. The Aeronautics Journal 108, 541–563.

De Moura, M.F.S.F., Gonçalves, 2004. Modelling the interaction between matrix cracking and delamination in carbon-epoxy laminates under low velocity impact. Composites Science and Technology 64, 1021–1027.

Finn, S.R., Springer, G.S., 1993. Delaminations in composite plates under transverse static or impact loads. Composite Structures 23, 177–204.

Guinard, S., Allix, O., Guédra-Degeorges, D., Vinet, A., 2002. A 3D damage analysis of low-velocity impacts on laminated composites. Composite Science and Technology 62, 585–589.

Hou, J.P., Petrinic, N., Ruiz, C., 2001. A delamination criterion for laminated composites under low-velocity impact. Composite Science and Technology 61, 2069–2074.

Kwon, Y.S., Sankar, B.V., 1993. Indentation flexure and low velocity impact damage in graphite epoxy laminate. Journal of Composite Technology and Research 15 (2), 101–111.

Ladevèze, P., Lubineau, G., Marsal, D., 2006. Towards a bridge between the micro- and mesomechanics of delamination for laminated composites. Composite Science and Technology 66, 698–712.

Lammerant, L., Verpoest, I., 1996. Modelling of the interaction between matrix cracks and delaminations during impact of composite plates. Composites Science and Technology 56, 1171–1178.

Li, S., Reid, S.R., Zou, Z., 2006. Modelling damage of multiple delaminations and transverse matrix cracking in laminated composites due to low velocity lateral impact. Composites Science and Technology 66, 827–836.

Mi, Y., Crisfield, M.A., Davies, G.A.O., 1998. Progressive delamination using interface elements. Journal of Composite Materials 32 (14), 1246–1272.

Petit, S., Bouvet, C., Bergerot, A., Barrau, J.J., 2007. Impact and compression after impact of a composite laminate with a cork thermal shield. Composites Science and Technology 67, 3286–3299.

Renault, M., 1994. Compression après impact d'une plaque stratifiée carbone époxyde – Etude expérimentale et modélisation éléments finis associée. Rapport interne EADS CCR.

Sztefek, P., Olsson, R., 2008. Tensile stiffness distribution in impacted composite laminates determined by an inverse method. Composites Part A 39 (8), 1283–1293.

Whitney, J.M., Nuismer, R.J., 1974. Stress fracture criteria for laminated composites containing stress concentrations. Journal of Composite Materials 8, 253–265.